

Quantitative and Qualitative Characterization of Coatings Added to Low Voltage Switches

Leila Troudi^{*}, Khaled Jelassi

Université de Tunis El Manar, Ecole Nationale d'Ingénieurs de Tunis,
LR11ES15 Laboratoire des Systèmes Électriques, Tunisia

Received 23 November 2021; received in revised form 13 March 2022; accepted 14 March 2022

DOI: <https://doi.org/10.46604/aiti.2022.8971>

Abstract

Electroplating is one of the most important processes in the manufacturing of switches. Coating the conductive parts of switches improves their appearance and increases their durability, even in severe environments. This study proposes a non-destructive testing method to qualitatively and quantitatively characterize coatings added to the conductive parts of low voltage switches (contacts and terminals). The method is based on the injection of a high-frequency signal into a switch using the vector network analyzer (VNA). An in-depth analysis of the reflected signal is conducted to characterize the coatings. For the quantitative characterization, a comparison is made between switches that are plated with different coating thicknesses. As for the qualitative characterization, a comparison is made between switches that are manufactured with different types of metals. The results show that each switch type has an electromagnetic signature that varies according to the conductivity and the thickness of the metals used for coating.

Keywords: electroplating, switches, scattering parameters, vector network analyzer, coatings

1. Introduction

Electroplating is the process of adding a metal coating to a metal [1]. The added coating can improve the metal's final characteristics, such as its corrosion resistance, surface hardness, friction resistance, surface texture, electrical characteristics, durability, etc. [2-3].

For example, nickel is used for corrosion protection and to enhance wear resistance [4]. It is generally used as an undercoat between the base metal and the added layer of coating to prevent the migration of the base metal to silver and gold coatings [5-6]. Silver is used because of its high electrical conductivity and its resistance to corrosion and oxidation [7]. In addition, it can reduce skin effect losses at high frequencies [8]. Copper is used because of its high conductivity and its ability to make the surface of the base metal smoother and ready for other coatings [9]. Gold is used to increase the lifetime and the stability of electrical performance because it is characterized by excellent resistance to corrosion, even in polluted environments [10].

When it comes to the application of electroplating, manufacturers face many challenges. First, it is difficult to guarantee the final result of electroplating, such as the nature, thickness, and proper application of coatings to the conductive parts of a switch, especially when using noble metals, which increases the manufacturing cost. If the different parts of a switch are assembled and a defect is found, it is difficult, if not impossible, to detect the flaw. Another industrial problem is the existence of components in the same production location that have the same exterior appearance but are manufactured with different types of coatings, such as gold-plated copper contacts and gold-plated silver contacts, or with different coating thicknesses, such as a plated component with a 0.6 μm thick gold layer and a plated component with a 1.3 μm thick gold layer.

^{*} Corresponding author. E-mail address: leila.troudi@enit.utm.tn

To overcome these problems, there are many non-destructive testing methods to qualitatively and quantitatively characterize metallic coatings. The most commonly used non-destructive testing methods are magnetic induction, eddy current, and radiometric methods (X-ray fluorescence and backscatter β), which are very expensive [11].

X-ray fluorescence allows the coating thickness to be measured with high precision, but it is very expensive [12]. This method is applied to coatings whose atomic number is greater than or equal to 11 [13]. Backscatter β is applied when the difference between the atomic number of the coating and that of the substrate is greater than 20% [14]. This is the case for copper ($Z = 29$), gold ($Z = 79$), and silver ($Z = 47$), but the measurements become complicated when nickel ($Z = 28$) is used as an undercoat. Magnetic induction is used to measure non-magnetic coatings on ferrous substrates and magnetic coatings on non-magnetic substrates [15]. It is applied to measure thicknesses between 0.001 mm and 1 mm [16]. Eddy current methods are applied to measure the thickness of non-conductive coatings on non-magnetic metallic substrates [17].

There are also destructive testing methods, such as microscopic analysis (optical microscopy or electron microscopy). These require the implementation of transverse cuts at the level of the conductor to be diagnosed. Then, the sections are analyzed using an optical system (optical microscope or scanning electron microscope) to obtain the appropriate magnification to determine the nature and thickness of coatings [18].

All the methods mentioned above for the characterization of coatings are only applied off the production line and make the final product unusable. This study presents a non-destructive testing method to characterize coatings added to the conductive parts of switches. To apply this method, a very high-frequency signal is injected into the switch to be tested. To ensure the transfer of the high-frequency signal without loss and distortion, the switch is mounted on a printed circuit board that is directly connected to the vector network analyzer (VNA). Then, the obtained signals (transmitted/reflected) are analyzed for the quantitative and qualitative characterization of coatings added to low voltage switches.

2. Description of the Proposed Solution

The proposed method to characterize coatings added to the conductive parts of switches (terminals and contacts) is based on the injection of a high-frequency signal into the device being tested to detect defects. The proposed prototype to carry out the different experimental tests is presented in Fig. 1(a). All parts of this prototype are detailed in Fig. 1(b).

A toggle switch is composed of two terminals, a central support, a movable contact that ensures the opening and closing of an electrical circuit, and a non-conductive housing. All the switches that were used during the experimental tests are shown in Table 1. A printed circuit board is formed by three transmission lines that are separated by a well-determined distance, which is equal to the distance between the central support and the terminals to connect the switch to the transmission lines. A SubMiniature version A (SMA) connector is put at the end of each transmission line to connect the board to the VNA. During the experimental tests, only two SMA connectors were used to make the connection between the printed circuit board and the VNA. The third connector is used if one of the SMA connectors is damaged.



(a) The experimental prototype

(b) Different parts of the experimental prototype

Fig. 1 The proposed prototype

Table 1 Tested switches

Number	Bipolar switches				Unipolar switches		
	10	10	10	5	5	9	7
Metal used	Silver (S)	Gold plated silver (GS)	Gold plated copper (GC)	GC with silver contact (GS silver contact)	GS with silver contact (GS silver contact)	GC with 1.3 μm gold coating thickness (GC, 1.3 μm)	GC with 0.6 μm gold coating thickness (GC, 0.6 μm)

The VNA is connected to the two transmission lines to inject the high-frequency signal into the switch. It generates a high-frequency signal that is injected into the device undergoing testing, and then detects the reflected and transmitted waves to calculate the S parameters [19].

The S parameters, also called scattering or dispersion parameters, address the main problem of experimental characterization of a two-port network at high frequencies. The determination of classical parameters, such as impedance Z, admittance Y, and ABCD parameters requires short, open circuits, which are very difficult to achieve at high frequencies [20-21]. For a two-port network, four parameters are calculated: S_{11} (reflection coefficient at port 1), S_{12} (transmission coefficient from port 2 to port 1), S_{21} (transmission coefficient from port 1 to port 2), and S_{22} (reflection coefficient at port 2).

The measured S_{11} parameters are analyzed using an AWR Design Environment that generates and reads touchstone files and plots the obtained results to distinguish between switches manufactured with different types of metals (silver, gold-plated silver (GS), and gold-plated copper (GC)). Then, to quantitatively and qualitatively characterize the coatings, the return losses of each switch type are calculated and presented in the form of a boxplot diagram, using MATLAB. The experimental tests are carried out in a frequency band that varies between 0.01 GHz and 10 GHz.

The return losses (RL), given by Eqs. (1) and (2) and expressed in decibels (dB), describe the power reflected from the incident power by the device being tested [22]. When the reflected power increases, the return losses (dB) decrease, and when the reflected power decreases, the return losses (dB) increase [23]. If the return losses (dB) $\rightarrow \infty$, the signal transmission is considered ideal; that is, there is no reflection. The return losses are defined by the following equation:

$$RL(dB) = 10 \log \left(\frac{P_{incident}}{P_{reflected}} \right) \quad (1)$$

The calculation of the return losses using the S_{11} parameter is expressed as:

$$RL(dB) = -20 \log_{10} |S_{11}| = -S_{11}(dB) \quad (2)$$

3. Experimental Results: Observations and Analysis

3.1. Comparison between the S_{11} parameters of the switches

The S_{11} parameters of the silver, GS, and GC switches are compared to qualitatively characterize the switches. Fig. 2 and Fig. 3 show that the S_{11} parameters of switches made with the same type of metal have the same curve shape. The curves are relatively similar, particularly the blue curves of the GS switches and the silver switches. Each type of switch is characterized by its specific S_{11} parameters.

Fig. 2 presents a comparison between the S_{11} parameters of silver switches and GC switches. In this case, the switches could be distinguished by the silver and gold colors. The measurements of the S_{11} parameters confirm this distinction through the differences between the S_{11} parameters of silver switches and those of GC switches at frequencies between 2 GHz and 4 GHz.

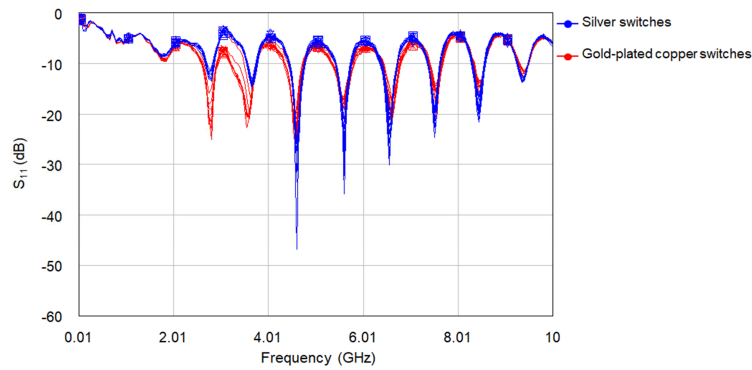


Fig. 2 S_{11} parameters of the silver switches and the GC switches

Fig. 3 shows a comparison between the S_{11} parameters of GS switches and GC switches. These switches have the same external appearance and therefore their characterization is very difficult. Both types of switches are gold-plated, but their difference can be observed when comparing the S_{11} parameters, which enables qualitative characterization of the switches without opening or disassembling them.

The differences between the S_{11} parameters are due to the proportional relationship between the reflection losses (S_{11}) and the conductivity of the metals. The conductivity of silver is higher than that of copper, so the reflection losses of silver are greater than those of copper [24]. The curves of the S_{11} parameters are relatively similar for the GS switches and the silver switches due to the presence of silver in both switches, as shown in Fig. 4.

The terminals and contacts of the switches are generally made of the same type of metal; that is, both are made of either silver, GS, or GC. In this part, two different types of metals are used in the same switch to determine the influence of this change on the performance of the switches.

Fig. 5 and Fig. 6 show the S_{11} differences between the GS switches and the GS switches with silver contacts, as well as the S_{11} differences between the GC switches and the GC switches with silver contacts, respectively. These differences are due to the use of different metals in the same switch.

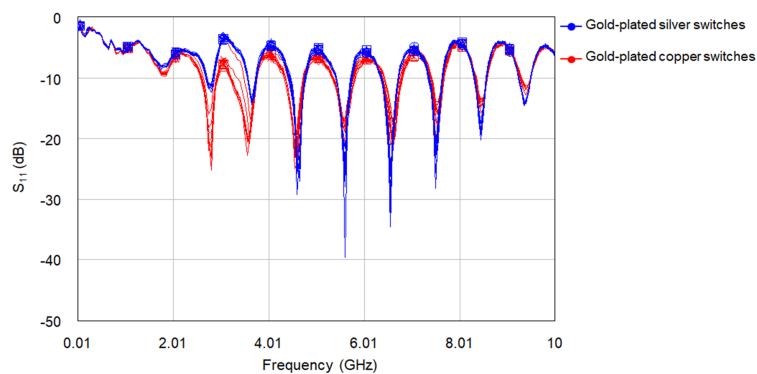


Fig. 3 S_{11} parameters of the GS switches and the GC switches

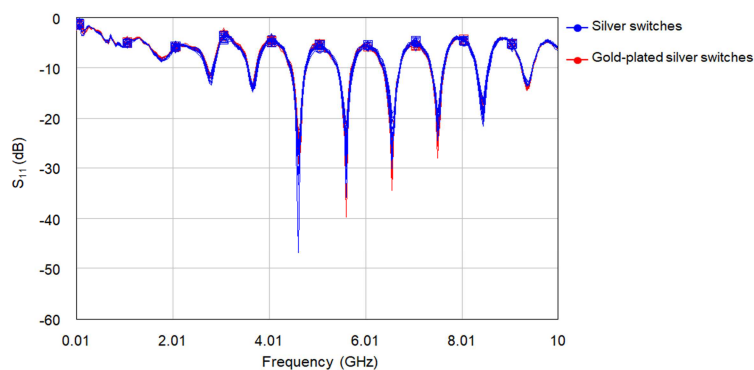


Fig. 4 S_{11} parameters of the silver switches and the GS switches

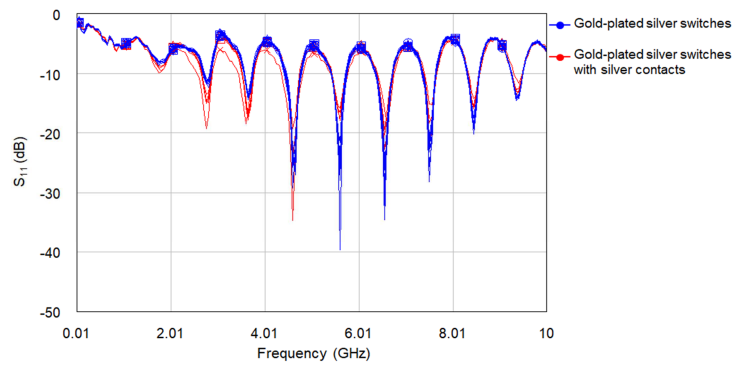


Fig. 5 S_{11} parameters of the GS switches and the GS switches with silver contacts

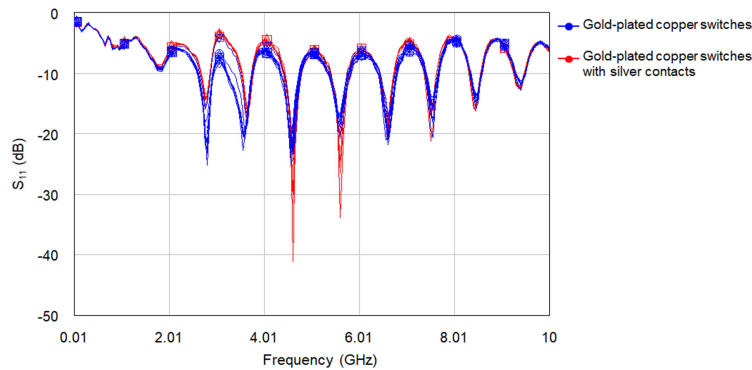


Fig. 6 S_{11} parameters of the GC switches and the GC switches with silver contacts

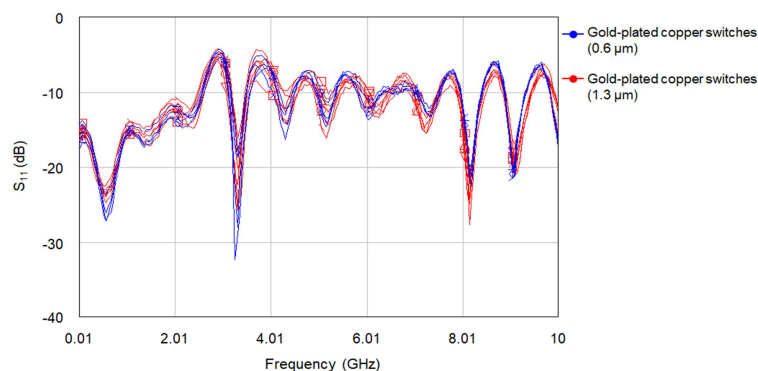


Fig. 7 S_{11} parameters of the GC switches with 0.6 μm and 1.3 μm coating thickness

Fig. 7 shows differences between the S_{11} parameters of GC switches with a coating thickness of 0.6 μm and GC switches with a coating thickness of 1.3 μm , particularly at frequencies between 8 GHz and 10 GHz. This result indicates that the thickness of the gold layer influences the electromagnetic signature of the switches.

3.2. Comparison between the return losses of the switches

To identify the causes of the differences between the S_{11} parameters of the different switches, the return losses of each switch group are calculated using Eq. (2). The obtained results are presented in the form of a boxplot diagram, which is a graphical representation of a statistical series and offers a quick and useful way to visualize the data distribution [25]. This graphical representation also allows the identification of measurement errors by symbols. The shapes of the curves are relatively similar, so the obtained signals are divided into several bands to plot the boxplot diagrams and to simplify the calculations.

In Figs. 8-10, differences in the return losses between switches appear in band 1 (frequency range: 0.01-1.8082 GHz), band 2 (frequency range: 1.8581-2.8072 GHz), band 3 (frequency range: 2.8571-3.5564 GHz), and band 4 (frequency range: 3.6064-4.5554 GHz). The current flows through gold and a small portion of copper or silver because, at high frequency, the current flows through the layer closest to the surface of the conductor. This is the case for the GC switches and GS switches.

Through a simulation using COMSOL Multiphysics, the current distribution is studied for a GC wire. The thickness of the gold layer is $1.3 \mu\text{m}$ and its boundaries are represented by white lines in Fig. 11. At 0.01 GHz and 1 GHz, the simulation results show that the current flows in the gold layer and a small portion of the copper layer, but at 10 GHz the current flows through the gold layer only [26]. This accounts for the differences between bands 1, 2, 3, and 4.

In Figs. 8-9, the return losses of the GC switches are greater than those of the GS switches and silver switches. At high frequencies, when the conductivity of metal increases, the reflection increases, and the return losses decrease [27-28]. For silver and GS switches, the difference is not very important because the current flows through the silver in the first four bands for both switches, as shown in Fig. 10.

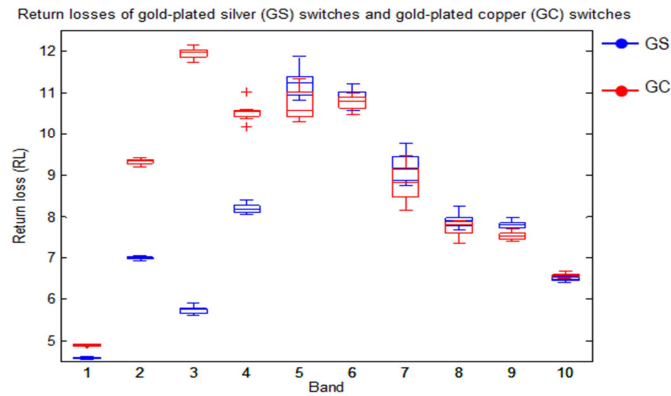


Fig. 8 Comparison between the return losses of the GS switches and the GC switches

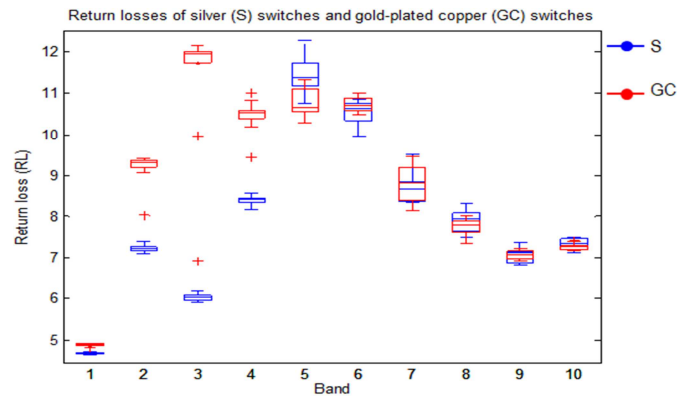


Fig. 9 Comparison between the return losses of silver switches and the GC switches

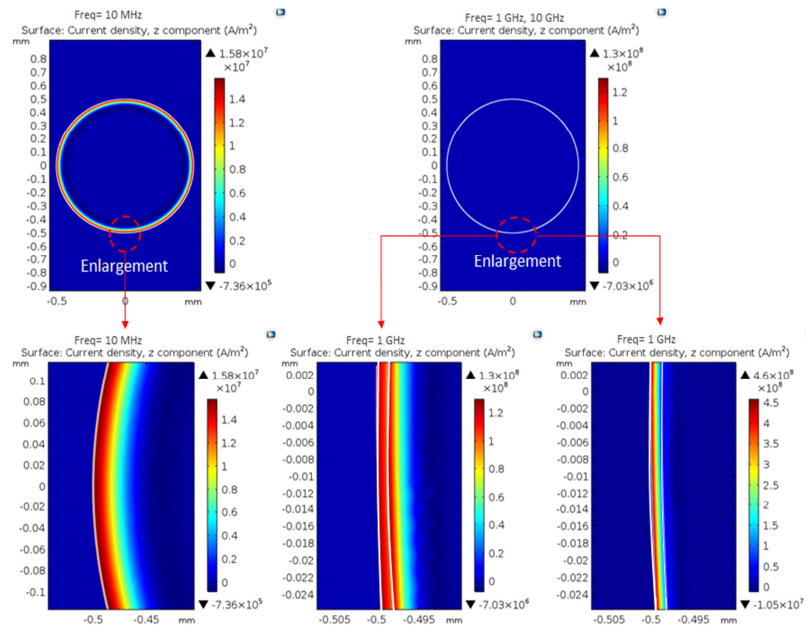


Fig. 10 Comparison between the return losses of silver switches and the GS switches

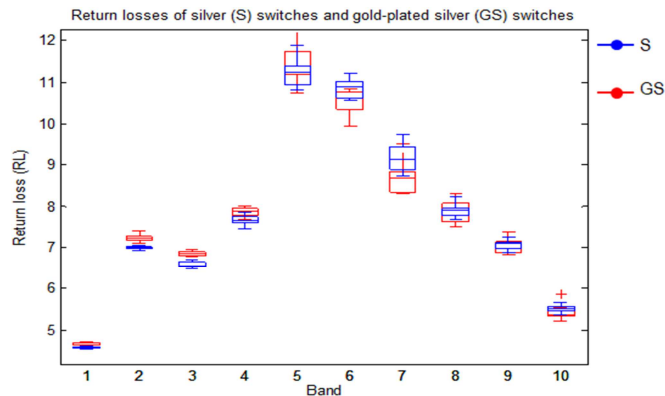


Fig. 11 Simulation on COMSOL Multiphysics to study the current distribution in a GC wire

From band 5 to band 10, the boxplots of the different switch types overlap. For the qualitative characterization of switches that have the same external appearance, such as GS switches and GC switches, it is sufficient to calculate the return losses in the first four bands, where the frequency varies between 0.01 GHz and 4.55545 GHz.

The connection between the movable contact and the terminal ensures the flow of the current through the switch, as shown in Fig. 1(b). When a silver contact is used instead of a GC contact for the GC switches, or instead of a GS contact for the GS switches, the return losses show large variation throughout the signal, as shown in Fig. 12 and Fig. 13. In this case, two different metals (gold and silver) are in contact. These results demonstrate that this contact between two different metals creates significant differences in the return losses of the switches.

Galvanic corrosion can result from the contact between two dissimilar metals. Each metal has a standard electrode potential. To avoid corrosion, the absolute value of the difference between the electrode potentials of two metals in contact should be very small [29].

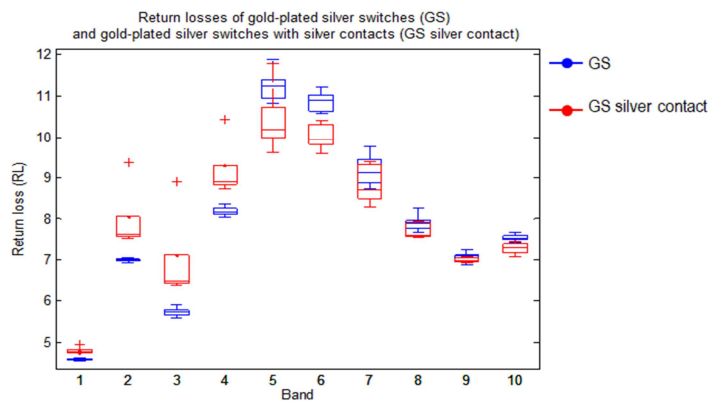


Fig. 12 Comparison between the return losses of the GS switches and the GS switches with silver contacts (GS silver contact)

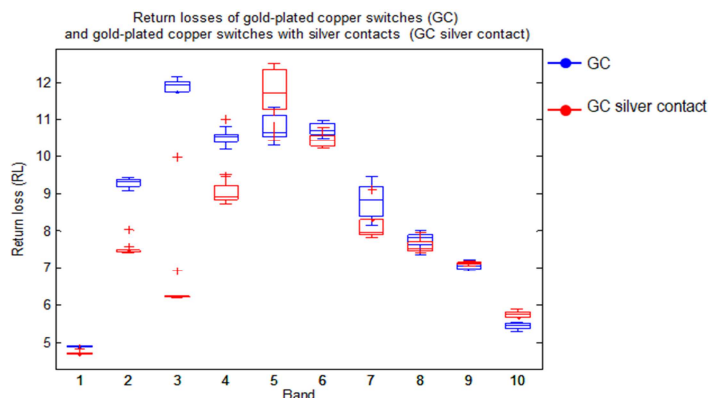


Fig. 13 Comparison between the return losses of the GC switches and the GC switches with silver contacts (GC silver contact)

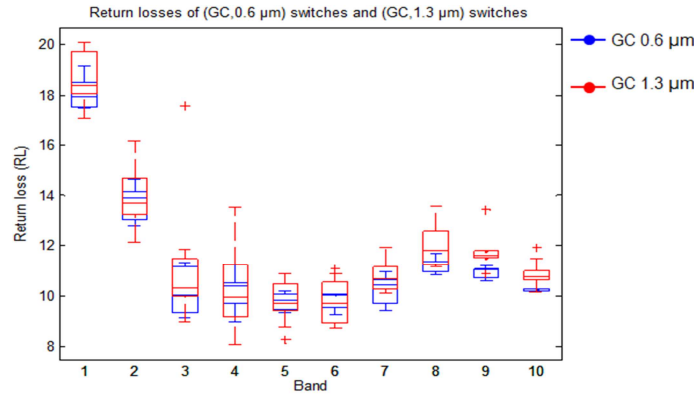


Fig. 14 Comparison between the return losses of the GC switches with 1.3 μm and 0.6 μm coating thickness

For example, the standard electrode potentials of copper, silver, and gold are equal to 0.16 V, 0.8 V, and 1.52 V, respectively. The difference between the potentials of silver and gold is 0.7 V and the difference between the potentials of gold and gold is 0.0 V. Therefore, the contact between gold and silver affects the electromagnetic signature of the GS switches with silver contacts (GS silver contact) and the GC switches with silver contacts (GC silver contact). Moreover, the obtained results could be used to identify the contact type in the assembled switches, especially over bands 2 and 3.

In Fig. 14, the boxplots of copper switches plated with a 0.6 μm thick gold layer (GC, 0.6 m) and copper switches plated with a 1.3 μm thick gold layer (GC, 1.3 m) are superimposed for frequencies between 0.01 GHz and 8.2018 GHz (from band 1 to band 8). At very high frequencies, because the current only flows through the gold layer, differences appear between the boxplots of the GC switches with 0.6 and 1.3 μm coating thickness in band 9 (frequency range: 8.2517-9.1009 GHz) and band 10 (frequency range: 9.1508-10 GHz). At high frequencies, the thickness of the upper layer of gold must be greater than the skin depth of the metal to avoid losses caused by the skin effect [30]. Therefore, the return losses of the GC switches with 1.3 μm coating thickness are greater than those of the GC switches with 0.6 μm coating thickness in bands 9 and 10, where the frequency varies between 8 GHz and 10 GHz.

The skin depth is calculated using the following equation:

$$\delta = \frac{1}{\sqrt{\pi f \sigma \mu}} \tag{3}$$

where μ is the permeability, σ is the conductivity, and f is the frequency. In bands 9 and 10, the skin depth of gold which is calculated using Eq. (3) varies between 0.7 μm and 0.8 μm, and the current flows through the gold layer only. Therefore, when the gold coating thickness increases, the reflection decreases, and the return losses increase.

4. Summary and Conclusions

This study presents an industrial non-destructive testing method for the qualitative and quantitative characterization of coatings added to low voltage switches. According to the proposed solution, which is based on the injection of a high-frequency signal into the switch to be tested, the types and thicknesses of coatings influence the electromagnetic signatures of switches.

When the conductivity of a metal increases, the reflection increases, and therefore the return losses decrease, which allows the qualitative characterization of switches. At high frequencies, the return losses of switches plated with a 1.3 μm thick gold layer are greater than those of switches plated with a 0.6 μm thick gold layer. The gold coating thickness must be greater than the skin depth of gold, which allows the quantitative characterization of switches. When the coating thickness is less than 0.6 μm, the accuracy of the proposed testing method decreases and the quantitative characterization of switches becomes difficult.

To summarize, the proposed testing method can be used to characterize coatings added to assembled, new, and used switches. It allows the characterization of coatings added to low voltage switches by the analysis of their reflected signals. To qualitatively characterize switches, the tests are carried out in a frequency range between 2 GHz and 4 GHz. For quantitative characterization, the tests are carried out in a frequency range between 8 GHz and 10 GHz.

Conflicts of Interest

The authors declare no conflicts of interest.

References

- [1] A. Mahapatro, et al., "Modeling and Simulation of Electrodeposition: Effect of Electrolyte Current Density and Conductivity on Electroplating Thickness," *Advanced Materials Science*, vol. 3, no. 2, pp. 1-9, August 2018.
- [2] B. Fotovvati, et al., "On Coating Techniques for Surface Protection: A Review," *Journal of Manufacturing and Materials Processing*, vol. 3, no. 1, Article no. 28, March 2019.
- [3] M. Tyagi, et al., *Optimization Methods in Engineering: Select Proceedings of CPIE 2019*, Singapore: Springer, 2020.
- [4] W. Sha, et al., *Electroless Copper and Nickel-Phosphorus Plating: Processing, Characterization, and Modeling*, Amsterdam: Elsevier Science, 2016.
- [5] S. Kyeong, et al., *Electrical Connectors: Design, Manufacture, Test, and Selection*, United States: John Wiley and Sons, 2021.
- [6] S. Roy, et al., *Advanced Surface Coating Techniques for Modern Industrial Applications*, United States: IGI Global, 2020.
- [7] D. Lu, et al., *Materials for Advanced Packaging*, 2nd ed., United States: Springer, 2017.
- [8] J. Moreira and H. Werkmann, *An Engineer's Guide to Automated Testing of High-Speed Interfaces*, 2nd ed., United States: Artech House, 2016.
- [9] C. Yang, et al., "Repairing the Specified Track on the Copper Coating Surface via Area-Selective Electrodeposition," *Journal of Materials Research*, vol. 36, no. 4, pp. 812-821, January 2021.
- [10] J. Song, et al., "Corrosion Protection of Electrically Conductive Surfaces," *Metals*, vol. 2, no. 4, pp. 450-477, December 2012.
- [11] F. I. Haider, et al., "A Comparison between Destructive and Non-Destructive Techniques in Determining Coating Thickness," *IOP Conference Series: Materials Science and Engineering*, vol. 290, no. 1, Article no. 012020, January 2018.
- [12] H. J. Streitberger, et al., *BASF Handbook Basics of Coating Technology: 3rd Revised Edition*, Germany: Hannover Vincentz Network, 2018.
- [13] K. Seshan, et al., *Handbook of Thin Film Deposition*, 4th ed., United States: Elsevier Science, 2018.
- [14] NPCS Board of Consultants and Engineers, *Electroplating, Anodizing, and Metal Treatment Hand Book*, India: Asia Pacific Business Press, 2003.
- [15] K. Gupta, *Micro and Precision Manufacturing*, Germany: Springer, 2017.
- [16] A. Errkik, et al., *Handbook of Research on Recent Developments in Electrical and Mechanical Engineering*, United States: IGI Global, 2019.
- [17] H. Brenig, "Non-Destructive Measurement of Coating Thicknesses," *IST International Surface Technology*, vol. 10, no. 1, pp. 60-61, 2017.
- [18] W. Giurlani, et al., "Measuring the Thickness of Metal Films: A Selection Guide to the Most Suitable Technique," *Materials Proceedings*, vol. 2, no. 1, Article no. 12, May 2020.
- [19] I. Llamas-Garro, et al., *Frequency Measurement Technology*, United States: Artech House, 2017.
- [20] D. S. Schmool, et al., "Single-Particle Phenomena in Magnetic Nanostructures," *Solid State Physics*, vol. 66, pp. 301-423, 2015.
- [21] M. Stănculescu, et al., "Using S Parameters in Wireless Power Transfer Analysis," *10th International Symposium on Advanced Topics in Electrical Engineering*, pp. 107-112, March 2017.
- [22] A. Singh, et al., "Design and Optimization of Microstrip Patch Antenna for UWB Applications Using Moth—Flame Optimization Algorithm," *Wireless Personal Communications*, vol. 112, no. 4, pp. 2485-2502, June 2020.
- [23] W. Boxian, et al., "Effect of Signal Reflection on the Performance of High-Density Ceramic Package Transmission Lines," *Journal of Physics: Conference Series*, vol. 1325, no. 1, Article no. 012170, October 2019.
- [24] M. F. Tai, et al., "EMI Shielding Performance for Varies Frequency by Metal Plating on Mold Compound," *Advances in Science, Technology, and Engineering Systems Journal*, vol. 2, no. 3, pp. 1159-1164, July 2017.

- [25] C. Thirumalai, et al., “Data Analysis Using Box and Whisker Plot for Lung Cancer,” *Innovations in Power and Advanced Computing Technologies*, pp. 1-6, April 2017.
- [26] L. Troudi, et al., “The Influence of the Coating Thickness on Transmission in Electronic Devices,” *10th International Renewable Energy Congress*, pp. 1-5, March 2019.
- [27] S. Varnaitë-Žuravliova, *The Types, Properties, and Applications of Conductive Textiles*, United Kingdom: Cambridge Scholars Publishing, 2019.
- [28] A. M. Chrysler, et al., “Effect of Material Properties on a Subdermal UHF RFID Antenna,” *IEEE Journal of Radio Frequency Identification*, vol. 1, no. 4, pp. 260-266, December 2017.
- [29] B. A. Omran, et al., *A New Era for Microbial Corrosion Mitigation Using Nanotechnology: Biocorrosion and Nanotechnology*, Switzerland: Springer Nature, 2020
- [30] H. Liu, et al., *High-Temperature Superconducting Microwave Circuits and Applications*, Singapore: Springer, 2019.



Copyright© by the authors. Licensee TAETI, Taiwan. This article is an open access article distributed under the terms and conditions of the Creative Commons Attribution (CC BY-NC) license (<https://creativecommons.org/licenses/by-nc/4.0/>).